HII-CHI-mistry: A collection of python scripts for the analysis of emission lines in ionized gaseous nebulae

Enrique Pérez-Montero

Instituto de Astrofsica de Andaluc a - CSIC. Apdo. 3004, 15080, Granada, Spain

1. General description

1.1. *What is* HII-CHI-mistry *and where can it be found?*

Ionized gaseous nebulae are ubiquitous objects in the Universe that provide valuable information about the galaxies where they reside through their bright emission lines. Among the various properties that can be derived from these nebulae are the relative chemical abundances of observed ions, the excitation of the gas, and the effective hardness of the ionizing source.

HII-CHI-mistry (hereafter, HCm) is a collection of Python scripts designed to analyze observational data from different bright emission lines measured in the ultraviolet, optical, or infrared ranges of the spectrum. By comparing these observations with predictions from extensive grids of photoionization models, HCm provides estimates and associated uncertainties for several derived properties, adapting the accuracy of the solutions based on the input lines and their uncertainties.

HCm offers three main advantages for the calculation of chemical abundances compared to other model-based solutions:

1. The results are fully consistent with the direct method, which relies on the prior determination of the electron temperature. This holds true even when the flux of an auroral line, such as [[O III]] λ 4363 Å, is not used (see Pérez-Montero, 2014). 2. HCm provides consistent solutions regardless of the set of input emission lines and their errors. This is particularly useful when comparing results for different sets of objects observed at different spectral ranges or redshifts. 3. HCm provides in a first step solutions for N/O (in the optical and infrared) or C/O (in the ultraviolet), allowing a later more accurate determination of O/H using N or C without assuming any prior relationship between O/H and N/O or C/O.

In this tutorial, I explain the features of the different versions of the code, their usage instructions, limitations, and expected future improvements. There are five versions of HCm depending on the spectral range and whether they are used for determining chemical abundances or calculating the hardness of the ionizing source. These versions are:

- HII-CHI-mistry: The original HCm package described in Pérez-Montero, 2014 for analyzing gaseous nebulae ionized by different sources of ionization including massive stars, active galactic nuclei, post-AGB stars or advected-dominated flows. It can be used to derive the total oxygen abundance (12+log(O/H), hereafter O/H), the nitrogen-to-oxygen chemical abundance ratio (log(N/O), hereafter N/O), and the ionization parameter (log U) using optical emission lines from [[O II]] λ 3727 Å up to [[S III]] λ 9069,9532 Å.

- HII-CHI-mistry-UV: Described in Pérez-Montero and Amorín, 2017 for star-forming objects, and in Pérez-Montero et al., 2023a for the NLR of AGN. It calculates O/H, the carbon-to-oxygen chemical abundance ratio (log(C/O), hereafter C/O), and log U, using ultraviolet emission lines from Lyα λ 1216 Å up to C III] λ 1909 Å.

• HII-CHI-MISTRY-IR: Described in Fernández-Ontiveros et al., 2021 for star-forming objects, and in Pérez-Díaz et al., 2022 for the NLR of AGNs. It estimates O/H, N/O, and log U using infrared emission lines from Brα λ 4.05 μm up to [[N II]] λ 205 μm.

• HII-CHI-MISTRY-TEFF: It calculates the equivalent effective temperature (T_{eff}) and log U using as input O/H and ratios of consecutive optical and UV emission lines, as described in Pérez-Montero et al., 2019b. It can also be used to derive the fraction of absorbed ionizing photons for objects with He II λ 4686 Å, as described in Pérez-Montero et al., 2020.

• HCM-TEFF-IR: It estimates T_{eff} and U based on near- and mid-infrared emission lines, as described in Pérez-Montero et al., 2024. It can also calculate the parameter α_{OX}, indicative of the hardness of the incident SED of AGN taking advantage of the very high-excitation lines present in this regime (see Pérez-Montero, submitted)..

HCM has been originally written in python v. 2.7, but from version 5 is only compatible with python 3. It can be downloaded from the HCM webpage at `http://home.iaa.es/~epm/HII-CHI-mistry.html`. In this document, I describe features for the public versions of HCM 5.5 and equivalent versions, which require the `Python` library `numpy`. Each package contains the corresponding script (with a `.py` extension), an `ASCII` file with instructions, an example input text file, and different libraries containing model information and template files for constrained sub-grids used by the code in the absence of certain emission lines. All files are included in a compressed `tgz` file, which can be uncompressed using the following command in a terminal prompt:

```
> tar xvfz HCm_v5.5.tar.gz
```

1.2. *How does the code work?*

All versions of HCM employ a Bayesian-like approach to derive chemical abundances, the ionization parameter, or T_{eff}. In brief, for a given property X, the final result is calculated as follows:

$$X_f = \frac{\sum_i X_i/\chi_i}{\sum_i 1/\chi_i} \tag{1.1}$$

where X_f is the final result, X_i are the input values from each model in the grid, and χ_i are the weights assigned to each model, calculated as the square difference of the observed and predicted values for specific emission-line ratios:

$$\chi_i^2 = \sum_j \frac{(O_j - T_{ji})^2}{O_j} \tag{1.2}$$

where O_j and T_{ji} are the observed and model-based values, respectively, for the considered emission-line dependent ratios. These ratios are described in each of the papers on the different versions of HCM as a function of the input emission lines. Notice that, contrary to a pure bayesian method, in which the model with the lowest χ^2 is selected, this method provides a more realistic estimation of the derived properties, even if the nominal values do not exactly match any of the models, but giving estimates for the corresponding uncertainties.

The errors assigned to each result are calculated as the square sum of two sources. The first is the dispersion of all results obtained through Monte Carlo iterations made by randomly perturbing the input nominal values with the input observational errors.

The second is the mean of all intrinsic uncertainties assigned to the Bayesian process, calculated as:

$$\Delta X^2 = \frac{\sum_i (X_f - X_i)^2 / \chi_i}{\sum_i 1/\chi_i} \tag{1.3}$$

For the versions of HCm aimed at calculating chemical abundances, the first iteration throughout the entire chosen grid of modelsprovides an estimation for the abundance of a secondary ion (N for HCm and HCm-IR, or C for HCm-UV), relative to oxygen. These estimations are based on emission-line ratios that are not very sensitive to $\log U$. This allows the grid to be constrained in a second iteration, once N/O or C/O are fixed, to calculate both O/H and $\log U$ using N or C lines without any prior assumption about the relationship between O and the respective secondary element.

In the case of HCm-Teff, both for the versions for the optical and the IR, this previous iteration is not performed. Instead the grid of models is interpolated to fix the value of O/H to the input value in order to minimize the dependence of both T_{eff} and U on metallicity.

2. HCm **in the optical**

2.1. *Running the program*

To run the HCm code version 5.5, type the following command in the terminal prompt:

```
> python HCm_v5.4.py
```

A description of the code will appear on-screen, prompting for the input file containing observational information. Alternatively, the input file name and the desired number of iterations for the Monte Carlo simulation can be specified when invoking the code:

```
> python HCm_v5.5.py input.txt 100
```

If the number of Monte Carlo iterations is not specified, it defaults to 25.

2.2. *The input file*

The input file must be an `ASCII` file, with as many rows as the number of objects or pointings for which the calculations are to be performed. Each column represents the identification for each row and the reddening-corrected fluxes relative to Hβ with their corresponding errors. In previous versions of HCm, all columns needed to be introduced, but from version 5.0 onwards, a first row with the labels of the introduced columns is required, and the order is not essential. The file can also include other columns not identified by the code. The columns dedicated to the observational relative errors are optional. The labels for the emission lines in this version are:

- `ID`: To identify each row with a name.
- `OII_3727` and `eOII_3727`: For [[O II]] λ 3727 Å and its error. Assumed to be the sum of λ 3726 Å and λ 3729 Å in resolved spectra.
- `NeIII_3868` and `eNeIII_3868`: For [[Ne III]] λ 3868 Å and its error.
- `OIII_4363` and `eOIII_4363`: For [[O III]] λ 4363 Å and its error.
- `OIII_4959` and `eOIII_4959`: For [[O III]] λ 4959 Å and its error.
- `OIII_5007` and `eOIII_5007`: For [[O III]] λ 5007 Å and its error. If only one of the two strong [[O III]] lines is provided, the code assumes the theoretical ratio between them.

- NII_5755 and eNII_5755: For [[N II]] λ 5755 Å and its error.
- SIII_6312 and eSIII_6312: For [[S III]] λ 6312 Å and its error.
- NII_6584 and eNII_6584: For [[N II]] λ 6584 Å and its error.
- SII_6716 and eSII_6716: For [[S II]] λ 6716 Å and its error.
- SII_6731 and eSII_6731: For [[S II]] λ 6731 Å and its error. Note that the code will only use the [[S II]] lines if both of them or their sum is provided.
- Alternatively, the sum of these two lines can be given as SII_6725 and eSII_6725.
- OII_7325 and eOII_7325: For [[O II]] $\lambda\lambda$ 7319+7330 Å and its error.
- SIII_9069 and eSIII_9069: For [[S III]] λ 9069 Å and its error.
- SIII_9532 and eSIII_9532: For [[S III]] λ 9532 Å and its error. If only one of the two strong [[S III]] lines is provided, the code assumes the theoretical ratio between them.

2.3. *Selecting the grid of models*

If the input file is correct, the code will prompt you to select the grid of models to perform the calculation:

```
(1) POPSTAR with Chabrier IMF, age = 1 Myr
(2) BPASS v.2.1 a_IMF = 1.35, Mup = 300, age = 1 Myr with binaries
(3) AGN, double component, α(UV) = -1.0
(4) pAGB NLTE models (Rauch 2003)
(5) Advected-dominated Accretion Flow for AGN (ADAF, Nemmen et al. 2014)

Other SED
(6) Different library

Choose SED of the models:
```

All grids have been calculated using the code Cloudy v.17 (Ferland et al., 2017) assuming a central ionizing source and a plane-parallel geometry. Grid 1 is described in Pérez-Montero, 2014 and is calculated using POPSTAR (Mollá et al., 2009) cluster model atmospheres with an instantaneous burst at an age of 1 Myr, assuming a Chabrier, 2003 initial mass function (IMF) and a constant electron density of 100 cm^{-3}. Grid 2 is described in Pérez-Montero et al., 2021 and was calculated with cluster model atmospheres from BPASS v.2.1 (Eldridge et al., 2017), assuming an instantaneous burst at an age of 1 Myr, an IMF with slope $x = -1.35$, an upper mass limit of 300 M$_\odot$, and binaries. The gas in these models has an electron density of 100 cm^{-3}. This grid is recommended for Extreme Emission Line Galaxies (EELGs).

Option 3 can be used to derive chemical abundances in the Narrow Line Regions (NLR) of AGN and includes several grids described in Pérez-Montero et al., 2019a. These assume a double-peaked power law spectral energy distribution with a parameter $\alpha_{UV} = -1.0$. The assumed electron density is 500 cm^{-3}. The code will ask for the value of α_{OX} with possible values from -0.8 to -2.0 in steps of 0.2, and the criterion used to stop the models (at an outer radius when the fraction of free electrons is 98% or 2%).

Models for post-AGB stars were calculated using libraries from Rauch, 2003 covering values for $T_{eff} = 5$, 10, and 15 $\cdot 10^4$ K, while models simulating advected-dominated flows (ADAFs) were taken from Nemmen et al., 2014. These two sets of models are available only from version 5.5 and they are described in Prez-Daz et al (submitted).

All default grids cover an input O/H value in the range [6.9, 9.1] in bins of 0.1 dex and N/O in the range [-2.0, 0.0] in bins of 0.125 dex. Log U is covered with a resolution of 0.25 dex in the range [-4.0, -1.5] for grids for star-forming regions (i.e., 1 and 2) and in the range [-2.5, -0.5] for grids for AGN. The user may also use their model libraries by including them as a text file in the correct format in the folder Libraries_opt. If a

different library is introduced by the user (4), the code will automatically check if the file has the correct format. If some information is missing, the code will warn the user about the missing columns.

Once the grid of models has been selected, the code will ask whether to use interpolation between the models in the grid:

`Choose models [0] No interpolation [1] Interpolation:`

In the interpolated mode, the code makes a linear interpolation of all variables, increasing the resolution by a factor of 10. This prevents the results from clustering around certain grid points. However, this mode slows the calculation time.

As a final step, the program will ask for the constraint laws to limit the grids. This is necessary when a limited set of emission lines is provided and the models must make assumptions about the relations between O/H and N/O (when N/O cannot be derived) or O/H and U (when no auroral line is provided, so excitation is used to estimate metallicity). For AGNs, there is a degeneracy of the O2O3 emission-line ratio, as discussed in Pérez-Montero et al., 2019a. To derive log U, the code will also ask for the preferred log U range for the calculations between high-ionization (log $U \geq$ -2.5) or low-ionization (log $U \leq$ -2.5).

`Select a file with the constraint laws to limit the grid of models when the measurement of a quantity is impossible without any relation.`

`Default constraints`

`(1) Constraints for Star-Forming Galaxies`
`(2) Constraints for Extreme Emission Line Galaxies`
`(3) Constraints for AGNs (no restriction on the ionization parameter)`
`(4) Constraints for high-ionization AGNs (log(U) > -2.5)`
`(5) Constraints for low-ionization AGNs (log(U) < -2.5)`

`Other constraints`

`(6) Different constraint file`

The user can also use their own constraint assumptions in a text file with the correct format in the folder `Constraints`. If option 6 is chosen, the code will check the file for the correct format. If some information is missing, the code will warn the user about the missing columns.

After this process, the program will summarize the different grids that will be used and the number of models for each grid. From version 5.4 onwards, this process can be sped up by changing the variable `interactive` from `True` to `False` in the script and editing the model parameters and constraints directly in the code.

2.4. *Results*

The code will display the results of the calculations for each row on the screen, along with the task's completeness ratio. At the end, an additional ASCII file containing all results will be generated, named the same as the input file but with the suffix `_hcm-output.dat`. The first column lists the identification of each row. If this was not specified in the input file, a number will be assigned. The next columns of this file contain the emission-line fluxes used as input, with their corresponding errors.

The next column is an index that indicates whether the whole grid of models has been used or if a constrained grid has been used instead. This depends mainly on the introduced
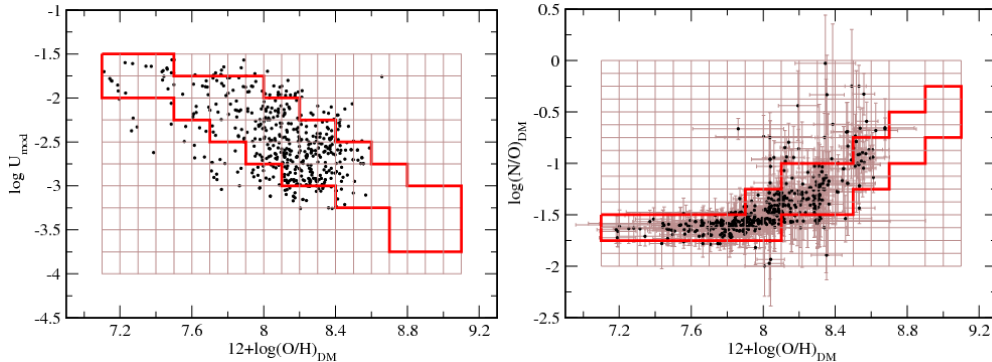
FIGURE 1. Left: relation between total oxygen abundance and ionization parameter for the sample studied in Pérez-Montero, 2014. The solid red line encompasses the most probable combination of parameters occupied by the objects. Right: empirical relation between 12+log(O/H) and log(N/O) with the region occupied by the grid of models in the absence of observational information to constrain N/O.

emission lines for each row, as a limited observational set implies additional assumptions to calculate ionic abundances. However, as described above, these constraints can be chosen based on the models, or the user can use their own. An index of 1 indicates that the whole grid of models has been used. This is done when an estimation of the electron temperature, similar to the direct method (see for instance Pérez-Montero, 2017), can be made because both auroral and nebular emission lines are present (e.g., [[O III]] 4363 Å with 4959, 5007 Å, [[N II]] 5755 Å with 6584 Å, [[O II]] 7325 Å with 3727 Å, or [[S III]] 6312 Å with 9069, 9532 Å). If any auroral line is not given, which is common in faint or metal-rich nebulae (Pérez-Montero and Díaz, 2005), additional assumptions should be made.

Index 2 represents the case when the electron temperature cannot be estimated, and the code assumes an empirical law between O/H and log U (see Figure 1). This relation assumes that metal-poor objects generally exhibit higher excitation, while metal-rich objects have lower excitation. This is the same assumption behind the use of many high- to low-excitation emission line flux ratios (e.g., O3O2, O3N2) to derive chemical abundances. Finally, index 3 denotes the use of a grid constrained by assuming an empirical relation between O/H and N/O, as shown in Figure 1. This is necessary when N/O cannot be calculated independently in a first iteration using emission-line ratios such as N2O2, O3N2, or N2S2. This assumption is behind all strong-line calibrations based on [[N II]] and implies a constant N/O value for low metallicities due to primarily primary production of N, and an increasing N/O with O/H when secondary production of N is assumed. This assumption can lead to non-negligible deviations from the real O/H if N/O does not lie in the expected regime, as discussed in Pérez-Montero and Contini, 2009.

The final six columns of the output file give the results for O/H, N/O, and log U with their corresponding errors. If no solution is found, O/H and log U are denoted by 0, and N/O is denoted by -10. If the code encounters an error for a specific row of the input, '9999' will be inserted in the output. In this case, the user should review the input lines or contact us for possible inconsistencies.

The results and consistency of the abundances derived from HCM for star-forming objects, whose abundances were derived from the direct method (Pérez-Montero, 2014), and for NLR in AGN as derived using detailed photoionization models (Pérez-Montero

TABLE 1. Mean offsets and standard deviation of the residuals of the resulting properties derived by HCm when the model from POPSTAR emission lines are used as input as a function of the used emission-line ratios. [[O III]]$_a$ stands for the [[O III]] auroral line at λ 4363 Å and [[O III]]$_n$ for the nebular lines at λ 4959, 5007 Å.

Used lines	Grid	O/H		N/O		log U	
		Mean Δ	σ res.	Mean Δ	σ res.	Mean Δ	σ res.
All lines	1	+0.03	0.09	-0.07	0.08	+0.06	0.15
[[O III]]$_a$,[[O III]]$_n$,[[N II]],[[S II]]	1	+0.02	0.09	-0.01	0.07	+0.06	0.15
[[O II]],[[O III]]$_n$,[[N II]],[[S II]]	2	-0.04	0.08	+0.00	0.03	+0.05	0.10
[[O III]]$_n$,[[N II]],[[S II]]	2	-0.03	0.07	+0.00	0.04	+0.05	0.10
[[O II]],[[O III]]$_n$,[[N II]]	2	-0.04	0.24	+0.00	0.23	+0.03	0.09
[[N II]],[[S II]]	2	+0.00	0.19	+0.00	0.04	+0.02	0.20
[[O III]]$_n$,[[N II]]	3	-0.04	0.08	–	–	+0.07	0.13
[[N II]]	3	+0.01	0.15	–	–	+0.03	0.21
[[O II]],[[O III]]$_n$	3	+0.00	0.01	–	–	+0.00	0.02
[[O II]],[[Ne III]]	3	-0.01	0.02	–	–	-0.01	0.03

et al., 2019a), are well discussed. Nevertheless, in Table 1, I provide a list of the mean offsets and the standard deviation of the residuals of the resulting O/H, N/O, and log U as compared with the input values from the models as a function of the used emission lines. These values illustrate how the code can recover the abundances from the values using only the emission lines as input, but cannot be taken as true uncertainties.

3. HCm in the ultraviolet

The HII-CHI-MISTRY-UV code (hereafter HCm-UV) is similar to the optical version but uses a different set of emission lines in the ultraviolet regime and estimates C/O instead of N/O in the first iteration. It also allows including two emission lines in the optical range to estimate the abundance based on an emission-line ratio sensitive to the electron temperature (e.g., [[O III]] λ 5007/λ 1665), although this may introduce larger inaccuracies due to reddening uncertainties. This code is described in Pérez-Montero and Amorín, 2017 for star-forming objects and in Pérez-Montero et al., 2023a for the NLR in AGN.

3.1. *Running the Program and Preparing the Input File*

Similar to the optical version, it can be executed from the terminal using Python, allowing the script to be run directly or with a specified input file and iteration count for Monte Carlo simulations:

```
> python HCm-UV_v5.0.py input.txt 100
```
The input file is an `ascii` file where the first row must contain labels for each column, including:
- `ID`: Identification name for each row.
- `Lya_1216` and `eLya_1216`: Lyα λ 1216 Å and its error.
- `NV_1239` and `eNV_1239`: N v] λ 1239 Å and its error.
- `CIV_1549` and `eCIV_1549`: C IV] λ 1549 Å and its error.
- `HeII_1640` and `eHeII_1640`: He IIλ 1640 Å and its error.

- OIII_1665 and eOIII_1665: [O III]] λ 1665 Å and its error. This includes all lines of the [O III]] multiplet between 1660 Å and 1666 Å.
- CIII_1909 and eCIII_1909: C III] 1909 Å and its error. Again, this includes all lines of the C III] multiplet.
- Hb_4861 and eHb_4861: Hβ λ 4861 Å and its error.
- OIII_5007 and eOIII_5007: [[O III]] λ 5007 Å and its error.

Subsequent rows should include identification names and extinction-corrected fluxes in arbitrary units. A value of zero can be used for missing values, and not all columns are required to estimate O/H, C/O, or U.

If the input file is correct, the code will prompt for the grid of models and the use of interpolation. Version 5.0 offers models from POPSTAR, BPASS, and double composite AGN. For AGN, the code will ask for the assumed α_{OX} (-0.8 or -1.2), the stopping criterion for the models (2% or 98

In the next step, the code will prompt for model interpolation to improve resolution and the choice of templates considering the assumed relation between O/H, log U, and C/O in case some input emission lines are missing. These templates can be edited by the user in the appropriate folder. As in the optical version, interactivity can be disabled by setting the variable `interactive` to `False`.

3.2. *Output File and Analysis of the Results*

Once the grid of models is selected, the code will display the results for each input row on the screen, along with the completeness ratio. At the end, it generates an output file in `ascii` format containing the results, including all information used for the calculations. The first column is the corresponding ID, and the next columns will be the input emission lines along with their errors.

The following column is an index indicating whether the complete model grid was used (index 1), which occurs only when both [[O III]] λ 1665 and 5007 Å are provided to estimate the electron temperature. Index 2 denotes a grid with an implicit relation between O/H and log U as shown in Figure 1. Finally, index 3 denotes a grid constrained by assuming a relation between C/O and O/H, similar to that shown in Figure 1 for N/O and O/H, considering a fixed C/N to the solar ratio. This index is applied when C/O cannot be calculated using the C3O3 emission line ratio, depending on C III] 1909 Å and [O III]] λ 1665 Å, but an estimate for both O/H and log U can be given using C lines. In any case, as commented above, this relation can be changed by the user in the folder `Libraries_uv`. The code, for instance, also provides the relation derived for EELGs given by Pérez-Montero et al., 2021.

The final six columns give the results for O/H, C/O, and log U with their corresponding errors. As in the case of the optical version, if no solution can be found for both O/H and log U, these are denoted as 0 in the file, and -10 for C/O. A value of 9999 appears when an error is detected in a specific row.

Table 2 lists the mean offsets and the standard deviation of the residuals when we use as input for the code the same predictions from the models of the grid, when POPSTAR models are used as a function of the different combination of emission lines that lead to a solution. A similar table for the results for AGN can be found in Pérez-Montero et al (2023).

4. HCm **in the infrared**

The program HII-CHI-MISTRY-IR (hereafter HCm-IR) calculates the total oxygen abundance, nitrogen-to-oxygen ratio, and ionization parameter using a set of observed

TABLE 2. Mean offsets and standard deviation of the residuals of the resulting properties derived by HCm-UV when the model from POPSTAR emission lines are used as input as a function of the used emission-line ratios.

Used lines	Grid	O/H		C/O		log U	
		Mean Δ	σ res.	Mean Δ	σ res.	Mean Δ	σ res.
All lines	1	+0.02	0.28	-0.05	0.08	+0.04	0.25
Lyα, C IV],He II,[O III]],C III]	2	+0.02	0.27	-0.06	0.19	+0.05	0.10
C IV],He II,[O III]],C III]	2	+0.10	0.30	-0.14	0.13	-0.11	0.20
Lyα,C IV],He II,C III]	3	+0.00	0.02	–	–	+0.00	0.01
C IV],He II,C III]	3	-0.01	0.03	–	–	+0.00	0.02

emission lines in the mid-infrared. As of version 3.1, the program also provides sulfur abundance estimates. It is described in Fernández-Ontiveros et al., 2021. Since version 3.0, the program also supports calculations for AGN narrow-line regions (NLR), as described in Pérez-Díaz et al., 2022.

4.1. *Running the Program and Preparing the Input File*

Similar to other versions, HCm-IR can be run from the terminal using Python, and the input text file and the number of Monte Carlo iterations can be specified in the same command:

```
> python HCm-IR_v3.1.py input.txt 50
```

The input file should be in `ascii` format, with the first row containing the row identifiers and emission line labels, using the following accepted labels:

- `ID`: Identification name for each row.
- `HI_4m` and `eHI_4m`: Paα at λ 4.07 μm and its error.
- `ArII_7m` and `eArII_7m`: [[Ar III]] at λ 6.98 μm and its error.
- `HI_7m` and `eHI_7m`: Brα at λ 7.46 μm and its error.
- `ArV_8m` and `eArV_8m`: [[Ar IV]] at λ 7.90 μm and its error.
- `ArIII_9m` and `eArIII_9m`: [[Ar III]] at λ 8.99 μm and its error.
- `SIV_10m` and `eSIV_10m`: [[S IV]] at λ 10.5 μm and its error.
- `HI_12m` and `eHI_12m`: Huα at λ 12.46 μm and its error.
- `NeII_12m` and `eNeII_12m`: [[Ne II]] at λ 12.8 μm and its error.
- `ArV_13m` and `eArV_13m`: [[Ar V]] at λ 13.1 μm and its error.
- `NeV_14m` and `eNeV_14m`: [Nev] at λ 14.9 μm and its error.
- `NeIII_15m` and `eNeIII_15m`: [[Ne III]] at λ 15.5 μm and its error.
- `SIII_18m` and `eSIII_18m`: [[S III]] at λ 18.8 μm and its error.
- `NeV_24m` and `eNeV_24m`: [Nev] at λ 24.3 μm and its error.
- `OIV_25m` and `eOIV_25m`: [OIV] at λ 25.9 μm and its error.
- `SIII_33m` and `eSIII_33m`: [[S III]] at λ 33.7 μm and its error.
- `OIII_52m` and `eOIII_52m`: [[O III]] at λ 52 μm and its error.
- `NII_57m` and `eNII_57m`: [[N II]] at λ 57 μm and its error.
- `OIII_88m` and `eOIII_88m`: [[O III]] at λ 88 μm and its error.
- `NII_122m` and `eNII_122m`: [[N II]] at λ 122 μm and its error.
- `NII_205m` and `eNII_205m`: [[N II]] at λ 205 μm and its error.

The program will then prompt for the model grid selection. For version 3.0, models from POPSTAR, BPASS, and double composite AGN are available. In the case of AGN,

TABLE 3. Mean offsets and standard deviation of the residuals of the resulting properties derived by HCM-IR when the models from POPSTAR emission lines are used as input as a function of the used emission-line ratios.

Used lines	Grid	O/H		N/O		log U	
		Mean Δ	σ res.	Mean Δ	σ res.	Mean Δ	σ res.
All lines	2	+0.04	0.09	-0.00	0.01	+0.02	0.07
[[Ne II]],[[Ne III]],[[S II]],[[S IV]],[[O III]],[[N II]],[[N III]]	2	+-0.03	0.13	+0.00	0.01	+0.02	0.07
[[O III]],[[N II]],[[N III]]	2	-0.01	0.18	+0.00	0.01	+0.02	0.15
HI,[[S III]],[[S IV]],[[Ne II]],[[Ne III]]	3	+0.04	0.04	–	–	-0.01	0.01
[[S III]],[[S IV]],[[Ne II]],[[Ne III]]	3	+0.04	0.04	–	–	+0.00	0.01
[[S III]],[[S IV]]	3	+0.02	0.02	–	–	+0.00	0.01
[[Ne II]],[[Ne III]]	3	+0.03	0.09	–	–	+0.00	0.06
[[N II]],[[N III]]	3	+0.00	0.11	–	–	+0.00	0.06

the code will ask for the assumed α_{OX} (-0.8 or -1.2), and the stopping criterion for the models (2% or 98% of free electrons). Additionally, as in other versions, users can include custom grids, by specifying them in the `Libraries_ir` folder. the code will prompt about model interpolation to enhance grid resolution by a factor of 10, though this may slow down calculations. Finally, the code will prompt for constraints when certain emission lines are missing. Again, the code can provide templates calculated for star-forming galaxies by Pérez-Montero, 2014, for EELGs by Pérez-Montero et al., 2021, or assuming low- or high-excitation AGNs. Additional constraint files can also be added by users, and the initial level of interactivity can be adjusted by setting the variable `interactive` in the script.

4.2. *Output File and Analysis of the Results*

As with previous versions of HCM, after selecting the model grid, the code will display results for O/H, N/O and log U. along with the ratio of completeness of the task. It will also create another `ascii` file whose first column is the identification of each row followed by the emission lines with their errors given as inputs. The next column indicates if the complete grid is used (index 1). However, as no auroral lines are available in this spectral range, this is not used in any case. The index 2 corresponds to the grid constrained following an empirical relation between O/H and log U, as shown in Figure 1. Finally, index 3 is used when no previous estimation of N/O, using the N3O3 parameter can be done, and an empirical relation between O/H and N/O is assumed as shown in right panel of Figure 1. Alternatively, these relations can be changed to EELGs or others defined by the user, as commented above.

Table 3 lists mean offsets and standard deviations of the residuals for the resulting O/H, N/O, and log U derived from the code from different sets of input emission lines, as compared with the values used as input in each grid of the model.

5. HCM **for the Calculation of** T_{eff}

The HII-CHI-MISTRY-TEFF (HCM-TEFF hereafter) differs from previous versions of HCM in its focus on calculating the effective temperature of the ionizing source (T_{eff}) and/or the fraction of absorbed ionizing photons, f_{abs}, assuming a matter-bounded geometry. This tool uses the relationship between the 'softness parameter' and the hardness

of the ionizing radiation (see Vilchez and Pagel, 1988, Pérez-Montero and Vílchez, 2009), as detailed in Pérez-Montero et al., 2019b and Pérez-Montero et al., 2020. A discussion on the impact of diffuse ionized gas (DIG) on results, particularly when low-excitation lines like [[S II]] are used, is presented in Pérez-Montero et al., 2023b. An independent version for the infrared, valid for the derivation of T_{eff} and U in star-forming regions, is described in Pérez-Montero et al., 2024. This same version permits the derivation of the shape of the incident field of radiation in the NLR of AGN, as described in Prez-Montero et al (submitted)..

5.1. *Running the Program and Preparing the Input File*

Running the program is equivalent to the previous versions of HCm, through the terminal prompt:

`> HCm-Teff_v5.2.py input.txt 50`

The input file, required in `ascii` format, begins with the object ID and labels of the emission lines, including, if available, the oxygen abundance, which helps reduce uncertainty. The code accepts the following labels:

- `ID`: Identification name for each row.
- `12logOH` and `e12logOH`: Total oxygen abundance $12+\log(O/H)$ and its error. This may be calculated using HCm in a previous iteration.
- `CIV_1549` and `eCIV_1549`: C IV] λ 1549 Å and its error.
- `CIII_1909` and `eCIII_1909`: C III] λ 1909 Å and its error. This should include all lines taking part in the multiplet around this wavelength.
- `OII_3727` and `eOII_3727`: [[O II]] λ 3727 Å and its error. As in the case of HCm, this represents the addition of the two lines of the doublet of [[O II]] if there is good spectral resolution.
- `OIII_4959` and `eOIII_4959`: [[O III]] λ 4959 Å and its error.
- `OIII_5007` and `eOIII_5007`: [[O III]] λ 5007 Å and its error. As in the case of HCm, if only one of the two lines of the [[O III]] doublet (4959, 5007) is introduced, the code assumes its addition taking into account its theoretical relation.
- `HeI_4471` and `eHeI_4471`: He I λ 4471 Å and its error.
- `HeI_5876` and `eHeI_5876`: He I λ 5876 Å and its error.
- `HeI_6678` and `eHeI_6678`: He I λ 6678 Å and its error.
- `HeII_4686` and `eHeII_4686`: He II λ 4686 Å and its error.
- `SII_6716` and `eSII_6716`: [[S II]] λ 6716 Å and its error.
- `SII_6731` and `eSII_6731`: [[S II]] λ 6731 Å and its error. It is also possible to use the addition of the two [[S II]] lines using `SII_6725` and `eSII_6725`.
- `SIII_9069` and `eSIII_9069`: [[S III]] λ 9069 Å and its error.
- `SIII_9532` and `eSIII_9532`: [[S III]] λ 9532 Å and its error. As in the case of [[O III]], if one of the two [[S III]] nebular lines is not introduced, the code assumes its addition taking the theoretical expected ratio.
- `ArIV_4740` and `eArIV_4740`: [Ar IV] λ 4740 Å and its error.
- `ArIII_7135` and `eArIII_7135`: [Ar III] λ 7135 Å and its error.
- `NII_6584` and `eNII_6584`: [[N II]] λ 6584 Å and its error.

The next rows in the input file should correspond to the different values for which the code should derive T_{eff} and log U. The provided emission line fluxes must be reddening corrected, but it is not necessary that they are relative to Hβ, as only ratios of lines of different ionization are used. Use 0 when no value is found for a line or error.

5.2. *The Grids of Models*

If the input file is correct and the variable `interactive` is set to `True` in the code, it will prompt the parameters we want to calculate:
```
(1) Effective temperature and ionization parameter
(2) Photon absorption fraction and ionization parameter

Choose derived parameters:
```

Depending on these parameters, the code will prompt for different grids of models and geometries. In the case of T_{eff}:
```
(1) WM-Basic (30-60 kK)
(2) WM-Basic (30-60 kK) and Rauch (80-120 kK) stellar atmospheres
(3) Black body (30-100 kK)

Choose models:
```

Option 1 calculates T_{eff} and $\log U$ using WM-Basic single star atmospheres from Pauldrach et al., 2001 from 30 to 60 kK, while option 2 extends the range up to 120 kK using post-AGB stellar atmospheres from Rauch. Option 3 uses black-body spectral energy distributions in the range 30-100 kK.

After selecting the model type, the program will prompt for the assumed geometry, given its impact on model positions within softness diagrams:
```
(1) Plane-parallel geometry
(2) Spherical geometry

Choose geometry of the models:
```

If we want to calculate the photon absorption factor, f_{abs}, defined as the ratio of ionizing hydrogen photons that do not escape from the nebula, along with $\log U$, this is calculated using cluster model atmospheres from BPASS v.2.1 from Eldridge et al., 2017, assuming an instantaneous burst at 4 Myr, with binaries and an IMF with slope $X = -1.35$ and an upper mass limit of 300 $M_\odot$. In this case, we can choose among models with stellar metallicity identical to that of the gas in each model, or either assume nearly metal-free stars ($Z = 10^{-5}$). The code also supplies models with black-body with $T_{eff} = 10^5$ K, equivalent for metal-free stars.
```
(1) BPASS cluster atmospheres, age = 4 Myr, Mup = 300, x = 1.35, w/binaries,
Z* = Zg
(2) BPASS cluster atmospheres, age = 4 Myr, Mup = 300, x = 1.35, w/binaries,
Z* = 1e-5
(3) Black-body, T* = 1e5 K
```

In this case, only spherical geometry models are considered.

In Figure 2, two examples of the behavior of the grids of models in one of the softness diagrams are shown, as in Pérez-Montero et al., 2020, illustrating how the grids of models cover the space of the emission line ratios.

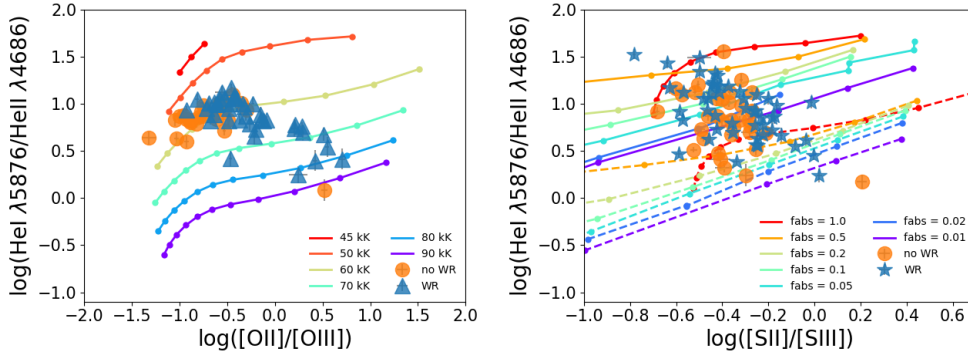Finally, the code will prompt for the possibility of using interpolation in the final chosen grid:

FIGURE 2. Examples of two softness diagrams for the sample of He II-emitters presented in Pérez-Montero et al., 2020. At left [[O II]]/[[O III]] vs He I/He II/ with models at 12+log(O/H) and different values for T_{eff} and, at right, using [[S II]]/[[S III]] and BPASS models assuming different values for f_{abs}. In all sequences values in the lower left part correspond to higher values for log U.

TABLE 4. Mean offsets and standard deviation of the residuals of the resulting properties derived by HCM-TEFF when the model emission lines are used as input as a function of the used emission-line ratios.

Used line ratios	T_{eff} (kK)†		log U^a		log f_{abs}‡		log U^b	
	Mean Δ	σ res.	Mean Δ	σ res.	Mean Δ	σ res.	Mean Δ	σ res.
[[O II]]/[[O III]], [[S II]]/[[S III]], He I/He II	+0.8	2.1	+0.01	0.10	+0.11	0.34	-0.10	0.53
[[O II]]/[[O III]], He I/He II	+0.8	2.1	+0.01	0.10	-0.12	0.27	+0.14	0.47
[[S II]]/[[S III]], He I/He II	+0.6	2.0	+0.03	0.13	-0.19	0.35	+0.10	0.62
[[S II]]/[[O III]], He I/He II	-0.3	5.1	+0.04	0.51	-0.07	0.27	-0.10	0.59
He I/He II	-0.5	6.8	+0.04	0.72	-0.12	0.35	-0.25.	0.63

```
Choose
```

5.3. *Output file and analysis of the results*

```
As in other versions of HCM, the code will show on the screen the results
for each row of the input file along with the ratio of completeness of the
task. At the end it will create an output file called as the name of the input
file adding _hcm-teff--ouput.dat. This file contains all the information for
the assumed grids and the results for each one of the rows.
```

  The first column lists the row identification, followed by input fluxes for each emission line, then the assumed O/H value (set to 0 if absent), and finally, the derived T_{eff} (or f_{abs} if Grid 3 is selected) and log U with associated errors. A value of 0 indicates that no solution was found due to insufficient line data, while -99999 signals an error with the specific input row.

  Table 4 lists the mean offsets and the standard deviation of the residuals for the obtained final results as a function of the input emission lines when compared with the input information from the code.

A similar code is available for its use based only on mid-IR emission-lines.
Although it is planned to merge it with the optical version, so far it workds
in an independent module. It is described and applied in Pérez-Montero et al.,
2024 to calculate T_{eff} for star-forming regions and in Pérez-Montero et al.
(submitted) to calculate α_{OX} in AGN, taking advantage of the high-excitation
lines that can be measured in this regime.

It basically works in the same way as it is described above, using exactly
the same grids of models with the exception of those calculated for the derivation
of the photon absorption factor. New models have been also calculated for AGN
in order to cover a wide range for α_{OX} in the range [-2.0,-1.0] and log U
in the range [-4.0,-1.0] for oxygen abundances from 12+log(O/H) from 8.1 to
9.0. The user can select for this modality between models with or without dust
grains mixed in the gas and test different stopping criteria in the models
(2%, 98%, and 99.9% of free electrons) what gives the possibility of exploring
the weight in the results of the low-excitation zone in the integrated spectrum.

The instructions and steps are the same, but using in the input the following
emission-lines, in addition to the ID and metallicity entries:

- ArIII_7m and ArIII_7m for [[Ar III]] at λ 6.98 μm and its error.
- ArIV_8m and ArIV_8m for [[Ar IV]] at λ 7.90 μm and its error.
- ArIII_9m and ArIII_9m for [[Ar III]] at λ 8.99 μm and its error.
- SIV_10m and eSIV_10m for [[S IV]] at λ at 10.5 μm and its error
- NeII_12m and eNeII_12m for [[Ne II]] λ 12.8 μm and its error.
- ArV_13m and ArV_13m for [[Ar V]] at λ 13.1 μm and its error.
- NeV_14m and eNeV_14m for [NeV] λ 14.9 μm and its error.
- NeIII_15m and eNeIII_15m for [[Ne III]] λ 15.5 μm and its error.
- SIII_18m and eSIII_18m for [[S III]] λ 18.8 μm and its error.
- NeV_24m and eNeV_24m for [NeV] λ 24.3 μm and its error.
- OIV_25m and eOIV_25m for [OIV] λ 25.9 μm and its error.
- SIII_33m and eSIII_33m for [[S III]] λ at 33.7 μm and its error.
- OIII_52m and OIII_52m for [[O III]] λ 52 μm and its error.
- NII_57m and eNII_57m for [[N II]] λ 57 μm and its error
- OIII_88m and eOIII_88m for [[O III]] λ 88 μm and its error
- NII_122m and eNII_122m for [[N II]] λ 122 μm and its error.
- NII_205m and eNII_205m for [[N II]] λ 205 μm and its error.

In this case, the code uses as observables ratios of low- to -high-ionization
IR emission-lines that can also be used to construct the corresponding IR softness
diagram (e.g. [[Ne II]]/[[Ne III]], [[S III]]/[[S IV]]). As compared to the optical
version, this version is less affected by DIG contribution as it involves higher
excitation emission-lines.

The very high excitation lines, such as [[O IV]] or [[Ne V]] can also be used
to discriminate very hard incident SEDs. In the case of AGN the line ratios
can only be used to provide an estimate of the hardness when they involve very
high-excitation lines (e.g. ([[Ne II]]+[[Ne III]])/[[Ne V]] or [[O III]]/[[O IV]],
or ([[S III]]+[[S IV]])/[[O IV]]).

Acknowledgements

REFERENCES

Chabrier, G. (2003). The Galactic Disk Mass Function: Reconciliation of the Hubble Space Telescope and Nearby Determinations. *ApJl*, 586:L133–L136.

Eldridge, J. J., Stanway, E. R., Xiao, L., McClelland , L. A. S., Taylor, G., Ng, M., Greis, S. M. L., and Bray, J. C. (2017). Binary Population and Spectral Synthesis Version 2.1: Construction, Observational Verification, and New Results. *PASA*, 34:e058.

Ferland, G. J., Chatzikos, M., Guzmán, F., Lykins, M. L., van Hoof, P. A. M., Williams, R. J. R., Abel, N. P., Badnell, N. R., Keenan, F. P., Porter, R. L., and Stancil, P. C. (2017). The 2017 Release Cloudy. *RMxAA*, 53:385–438.

Fernández-Ontiveros, J. A., Pérez-Montero, E., Vílchez, J. M., Amorín, R., and Spinoglio, L. (2021). Measuring chemical abundances with infrared nebular lines: HII-CHI-MISTRY-IR. *A&A*, 652:A23.

Mollá, M., García-Vargas, M. L., and Bressan, A. (2009). PopStar I: evolutionary synthesis model description. *MNRAS*, 398:451–470.

Nemmen, R. S., Storchi-Bergmann, T., and Eracleous, M. (2014). Spectral models for low-luminosity active galactic nuclei in LINERs: the role of advection-dominated accretion and jets. *MNRAS*, 438(4):2804–2827.

Pauldrach, A. W. A., Hoffmann, T. L., and Lennon, M. (2001). Radiation-driven winds of hot luminous stars. XIII. A description of NLTE line blocking and blanketing towards realistic models for expanding atmospheres. *A&A*, 375:161–195.

Pérez-Díaz, B., Pérez-Montero, E., Fernández-Ontiveros, J. A., and Vílchez, J. M. (2022). Measuring chemical abundances in AGN from infrared nebular lines: HII-CHI-MISTRY-IR for AGN. *A&A*, 666:A115.

Pérez-Montero, E. (2014). Deriving model-based Tₑ-consistent chemical abundances in ionized gaseous nebulae. *MNRAS*, 441(3):2663–2675.

Pérez-Montero, E. (2017). Ionized Gaseous Nebulae Abundance Determination from the Direct Method. *PASP*, 129(974):043001.

Pérez-Montero, E. and Amorín, R. (2017). Using photo-ionisation models to derive carbon and oxygen gas-phase abundances in the rest UV. *MNRAS*, 467(2):1287–1293.

Pérez-Montero, E., Amorín, R., Pérez-Díaz, B., Vílchez, J. M., and García-Benito, R. (2023a). Assessing model-based carbon and oxygen abundance derivation from ultraviolet emission lines in AGNs. *MNRAS*, 521(1):1556–1569.

Pérez-Montero, E., Amorín, R., Sánchez Almeida, J., Vílchez, J. M., García-Benito, R., and Kehrig, C. (2021). Extreme emission-line galaxies in SDSS - I. Empirical and model-based calibrations of chemical abundances. *MNRAS*, 504(1):1237–1252.

Pérez-Montero, E. and Contini, T. (2009). The impact of the nitrogen-to-oxygen ratio on ionized nebula diagnostics based on [NII] emission lines. *MNRAS*, 398:949–960.

Pérez-Montero, E. and Díaz, A. I. (2005). A comparative analysis of empirical calibrators for nebular metallicity. *MNRAS*, 361(3):1063–1076.

Pérez-Montero, E., Dors, O. L., Vílchez, J. M., García-Benito, R., Cardaci, M. V., and Hägele, G. F. (2019a). A bayesian-like approach to derive chemical abundances in type-2 active galactic nuclei based on photoionization models. *MNRAS*, 489(2):2652–2668.

Pérez-Montero, E., Fernández-Ontiveros, J. A., Pérez-Díaz, B., Vílchez, J. M., Kumari, N., and Amorín, R. (2024). Exploring the hardness of the ionising radiation with the infrared softness diagram. I. Similar effective temperature scales for starbursts and (ultra)luminous infrared galaxies. *A&A*, 684:A40.

Pérez-Montero, E., García-Benito, R., and Vílchez, J. M. (2019b). Revisiting the hardening of the stellar ionizing radiation in galaxy discs. *MNRAS*, 483:3322–3335.

Pérez-Montero, E., Kehrig, C., Vílchez, J. M., García-Benito, R., Duarte Puertas, S., and Iglesias-Páramo, J. (2020). Photon leaking or very hard ionizing radiation? Unveiling the nature of He II-emitters using the softness diagram. *A&A*, 643:A80.

Pérez-Montero, E. and Vílchez, J. M. (2009). On the hardening of the ionizing radiation in HII regions across galactic discs through softness parameters. *MNRAS*, 400:1721–1725.

Pérez-Montero, E., Zinchenko, I. A., Vílchez, J. M., Zurita, A., Florido, E., and Pérez-Díaz, B. (2023b). The softness diagram for MaNGA star-forming regions: diffuse ionized gas contamination or local HOLMES predominance? *A&A*, 669:A88.

Rauch, T. (2003). A grid of synthetic ionizing spectra for very hot compact stars from NLTE model atmospheres. *A&A*, 403:709–714.

Vilchez, J. M. and Pagel, B. E. J. (1988). On the determination of temperatures of ionizing stars in H II regions. *MNRAS*, 231:257–267.